SENSITIVITY OF OVERALL VEHICLE STIFFNESS TO LOCAL JOINT STIFFNESS

Choon T. Chon
Vehicle Methods and Components Department
Engineering and Manufacturing Staff
Ford Motor Company
Dearborn, Michigan

SUMMARY

The present paper discusses how overall vehicle stiffness is affected by local joint stiffness. By using the principle of virtual work and the minimum strain energy theorem, a closed form expression for the sensitivity coefficient has been derived. The insensitivity of the vehicle stiffness to a particular joint, when its stiffness exceeds a certain value (or threshold value), has been proved mathematically. In order to investigate the sensitivity of the structure to the joint stiffness, a so-called "stick" model has been created, and the modeling technique is briefly described. Some data on joint stiffness of tested vehicles are also presented.

INTRODUCTION

Over the years, the study of the joint behavior of vehicle structures has been identified as one of the most important subjects in the automotive industry. It is widely known that the flexibility of structural joints can affect not only the NVH (Noise, Vibration and Harshness) characteristics of the vehicle, but also other vital structural performance characteristics under various loading conditions (e.g. crash loads, road loads, jacking load, towing load, etc.).

The first study which accounted for the effect of flexible joints on automotive structural responses was by Chang [1] who used a two-dimensional frame model for a static analysis. He found that the structural response is far more sensitive to reducing joint stiffnesses (relative to the baseline values) than to increasing them. Recently a similar phenomenon was reported by Du and Chon [2], and it was claimed that there might exist a threshold stiffness value in a given joint of a vehicle structure. In other words, if a joint stiffness exceeds the threshold value, then the overall stiffness of the structure becomes insensitive to the particular joint.

The objective of the present paper is to demonstrate this phenomenon theoretically by showing that the derivative of the total strain energy with respect to a particular joint stiffness decreases and becomes zero as the joint stiffness approaches infinity. It should be noted that under the same loading and boundary conditions, the structure which contains higher strain energy is less stiff than the structure with lower strain energy. In this paper, a closed form expression for the sensitivity coefficient has been derived, using the principle of minimum strain energy and the principle of virtual work. In order to investigate the sensitivity of the structure to joint stiffness, a so-called "stick" model has been created, and the modeling technique is described. The last section discusses joint behavior, in general, by comparing the analytical results with test data. Discussion of other component behavior is also given based on the sensitivity coefficients derived in the paper.

SYMBOLS

p_i	generalized force vector
Q_j	generalized stress vector
u_i	generalized displacement vector
q_j	generalized strain vector
S	surface of the structure
S_p	surface where the force vector, p_i, is prescribed
S_u	surface where the displacement vector, u_i, is prescribed
D_{jk}	compliance matrix
U	total strain energy
Q_j^w	free component of Q_j
Q^r	reactant component of Q_j
N_r	total number of redundancies
b_m	m-th parameter
N_b	total number of parameters
n_ℓ	vector normal to the boundary surface S as shown in Fig. 1
V_m	volume in which D_{jk} depends on b_m.

U_m strain energy stored in the volume V_m due to the external loads p_i

J_m m-th joint stiffness

U_s total strain energy stored in a "stick" model under prescribed loading conditions

U_{sm} strain energy stored in the m-th joint under given external loads

N number of joints

α_p joint stiffness multiplication factor

BASIC CONCEPTS

This section summarizes the basic concepts of the general sensitivity study reported in Refs. [3.5]. They will then be applied to joint behavior in the later section.

(i) THEORETICAL BACKGROUND - Linearity of the equilibrium and strain-displacement relations will permit the principle of virtual work to be written as:

$$\int_V Q_j \, q_j^* \, dV = \int_S p_i \, u_i^* \, dS \tag{1}$$

where p_i and Q_j are any statically admissible fields, and u_i^* and q_j^* are any kinematically admissible fields. In the current paper, the body forces are assumed to be negligible. Note that $S = S_p + S_u$ (Fig. 1).

Let the solution of a structural problem for an elastic material be given by u_i, Q_j, and q_j. These quantities constitute, by definition, both a statically admissible field and a kinematically admissible field. In addition, q_j and Q_k satisfy Hooke's law:

$$q_j = D_{jk} \, Q_k \tag{2}$$

Note that if the deformations are small, the total strain energy stored in the loaded system will be equal to the work done by the applied forces. Thus the

total strain energy U may be expressed in terms of generalized stresses as:

$$U = 1/2 \int_V D_{jk} Q_j Q_k \, dV \tag{3}$$

Since a structure is, in general, statically indeterminate, one may divide the generalized stress $Q_j(x_\ell)$ at any point x_ℓ into two parts:

$$Q_j (x_\ell) = Q_j{}^w (x_\ell) + \sum_{r=1}^{N_r} \lambda_j{}^r(x_\ell) Q^r \tag{4}$$

where $\lambda_j{}^r (x_\ell)$ $(r = 1,\ldots,N_r)$ are linear functions of x_ℓ. Then substituting Eq. (2) into Eq. (1) and using the principle of virtual work (Eqs. (1) and (4)), one can prove that

$$\frac{\partial U}{\partial Q^r} = \int_V D_{jk} \lambda_j{}^r Q_k \, dV = 0 \tag{5}$$

Eq. (5) implies that the quantity U is minimized with respect to the values of each of the redundancies; Eq. (5) thus yields exactly N_r equations from which the values of the redundancies may be found.

(ii) SENSITIVITY ANALYSIS - The objective, then, is to derive a closed form expression for the sensitivity coefficient $\partial U/\partial b_m$. Differentiating the total strain energy, U, which is defined in Eq. (3), with respect to the m-th variable b_m, leads to the following expression:

$$\frac{\partial U}{\partial b_m} = 1/2 \int_S D_{jk} Q_j Q_k \frac{\partial x_\ell}{\partial b_m} n_\ell \, dS + 1/2 \int_V \frac{\partial D_{jk}}{\partial b_m} Q_j Q_k \, dV$$

$$+ \int_V D_{jk} \frac{\partial Q_j}{\partial b_m} Q_k \, dV \tag{6}$$

Here Eq. (6) may be considered as material derivative of volume integral [6].

Eq. (6) can be greatly simplified, if one chooses certain types of parameters. For example, an appropriate choice of cross-sectional properties (e.g., material property, area, moment of inertia, etc.) of either beam or

plate/shell structures, makes the first term of Eq. (6) identical to zero. And since the free components Q_j^w in Eq. (4) are the solutions of the statically determinate structures, they are independent of cross-sectional properties, which results in:

$$\frac{\partial Q_j}{\partial b_m} = \sum_{r=1}^{N_r} \lambda_j^r \frac{\partial Q^r}{\partial b_m} \tag{7}$$

Then using the minimum strain energy principle (Eq. (5)) and Eq. (7), it can be shown that the last term of Eq. (6) also vanishes. Finally one can rewrite Eq. (6) as:

$$\frac{\partial U}{\partial b_m} = 1/2 \int_{V_m} \frac{\partial D_{jk}}{\partial b_m} Q_j Q_k \, dV \tag{8}$$

It should be noted that the integration in Eq. (8) need only be performed over the region V_m in which D_{jk} depends on b_m.

In addition, if one can express the compliance tensor D_{jk} as inversely proportional to b_m (i.e., $D_{jk} \propto 1/b_m$) in the region V_m, then Eq. (8) can be further simplified:

$$\frac{\partial U}{\partial b_m} = -\frac{1}{b_m}\left(1/2 \int_{V_m} D_{jk} Q_j Q_k \, dV\right) = -\frac{U_m}{b_m} \tag{9}$$

VEHICLE STRUCTURAL MODEL

Before proceeding further, it is necessary to describe a vehicle structural model for the purpose of studying the sensitivity of local joint stiffness to the overall structural stiffness.

"STICK" MODEL - A "stick" model has been created according to the concept described in [2] (Fig. 2). This modeling concept is based on the assumption that beams/frames are the primary load carrying members in a structure.

The model consists of 188 grid points and 259 beam elements. Beams are modeled with proper offset vectors, which are often very useful when modeling beams containing eccentricity [7]. Even though there are no shell elements, per

se, several equivalent beam elements are introduced to simulate the sheet metal structures (e.g., floor panel, dashboard, wheel housing, rear quarter panel, etc.). By equivalent beam elements we mean that sectional properties are computed as if panels were beams. The Ford Computer Graphics System is used to create the model. The software for the Ford Graphics System is called PDGS (Product Design Graphics System) which is a general purpose three-dimensional design and drafting system. FAST (Finite element Analysis SysTem), which is embedded in PDGS, can be accessed from the main menu of the PDGS and allows the user to build and modify a finite element model.

TESTS - Bending and torsional tests were performed on the body structure in accordance with the Company Test Procedure. The structure was supported at the center of front and rear wheels. In order to apply the bending load across each seat position (so-called H-point), a heavy beam was laid on three points (on both left and right rocker panels and the middle tunnel) with spacers underneath so that the beam can be levelled with respect to the ground. The beam weighs 4,448.2 N (1,000 lb.). For the torsional test, the applied torque was 3.39×10^6 N-mm (2,500 ft-lb.) at both centers of the front wheels, while the rear wheel axle was supported.

ANALYSES - Elastic analyses under bending and torsional loads were performed using the "stick" model described above with the following boundary conditions and material properties.

Loading (L.C.) and Boundary (B.C.) Conditions :

(a) Static Bending Analysis

L.C. : Unit downward (-z direction) displacements are prescribed at both the right and left rocker panels, and the middle tunnel. This simulates the dead weight applied in the test setup and these points coincide with the H-point of the "stick" model. Since displacements are prescribed instead of forces as the loading condition, reaction forces at the loading points are computed, and the deflections are proportionally adjusted so that the sum of the reaction forces equals 4448.2 N (1000 lbs.).

B.C. : Simply supported at both the front and rear wheel centerlines with one end allowed to move freely in the x-direction.

(b) Static Torsional Analysis

L.C. : Two vertical loads, 4945.0 N (1111.7 lbs.) each, in opposite directions, which are equivalent to 3.39×10^6 N-mm (2500 ft-lb torque) were applied at the centerline of the front wheel axle.

B.C. : Simply supported at the centerline of the rear wheel axle.

Material and Cross-Sectional Properties:

Young's modulus (E) and Poisson's ratio (ν) used in the model are:

$$E = 2.07 \times 10^5 \ N/mm^2 \quad (30.0 \times 10^6 \ psi)$$

$$\nu = 0.3$$

ACCURACY OF THE MODEL - In this subsection, the analytical results were compared to the test data to investigate the accuracy of the model.

The overall deformed shapes obtained from the analyses and the tests for both bending and torsion are compared in Figs. 3a and 3b. The dotted and solid lines represent the test data and the analysis results, respectively. The abscissa denotes the x-coordinate of the body structure from the front to the rear wheel axles and thus represents the length of the wheel base. The ordinates denote normalized deflections for the bending analysis and twist angles for the torsional analysis. Note that these values were measured along the bottom rails of the structure in the actual test.

Even though the overall deformed shape from the analysis is in good agreement with that of the test, the analytical and test curves show a slight discrepancy in the rear of the vehicle. This may have resulted from the slight difference in the boundary conditions between the analysis and the test setup. The torsional curve from the analysis gives a good agreement with the test data. It should be noted that the curve obtained from the test data has more local fluctuation in magnitude. Studying the reasons of it is beyond the scope of this report.

A rationale which justifies the concept of a "stick" model approximation for predicting the overall stiffness of a vehicle structure is established in a separate paper*. In this paper, it is shown that the upper bounds as well as the lower bounds of total strain energy are the same for both the vehicle structure and the corresponding "stick" model.

SENSITIVITY STUDY OF JOINTS

Thus far, the basic concept of derivation of the sensitivity coefficients and the concept of the "stick" model approximation have been presented. This section

*Chon, C. T.: "Rationalization of "Stick" Model Approximation," work in progress.

describes the application of the above results to the sensitivity study of joints which affects the overall vehicle stiffness. As mentioned above, it has been analytically and experimentally demonstrated in [1 & 2] that the joint behavior is one of the most important factors for the overall stiffness of the body structure. For the sake of clarity, this section is divided into two subsections: the cases of a single joint and multiple joints.

A SINGLE JOINT - In the model analyzed, the joint which connects the rocker panel and the bottom of the B-pillar (see Fig. 4) was identified as the joint to which the total strain energy was most sensitive. This was done by comparing the amount of strain energy stored in the joints. After introducing a joint magnification factor which was used in [2] (see Fig. 4 for the joint locations), a parametric study of the joint behavior was performed. Fig. 5 shows how the total strain energy of the structure is affected by the joint stiffness of the B-pillar and the rocker panels. Note that the total strain energy becomes insensitive as the joint stiffness becomes large. This phenomenon can be explained using the sensitivity coefficient derived in the previous section (see Eq. (9)) as follows:

Let $b_m = J_m$ and let U_s be the total strain energy stored in the model under the prescribed loading conditions (either bending or torsion). Then Eq. (8) can be rewritten as:

$$\frac{\partial U_s}{\partial J_m} = 1/2 \int_{V_m} \frac{\partial D_{jk}}{\partial J_m} Q_j Q_k \, dV \tag{10}$$

Note that integration in Eq. (10) needs only be performed over the volume in which the m-th joint is contained. Moreover, since the compliance tensor D_{jk} is inversely proportional to the m-th joint stiffness, J_m, the final form of Eq. (10) is:

$$\frac{\partial U_s}{\partial J_m} = - \frac{U_{sm}}{J_m} \tag{11}$$

It is very important to note from Eq. (11) that the sensitivity coefficient $\partial U_s/\partial J_m$ goes to zero as the m-th joint stiffness, J_m, approaches infinity. Mathematically one can write this as:

$$\lim_{J_m \to \infty} \frac{\partial U_s}{\partial J_m} = \lim_{J_m \to \infty} \left(- \frac{U_{sm}}{J_m} \right) = 0 \tag{12}$$

Eq. (12) proves the phenomenon shown in Fig. 5 for a large value of J_m (see region "C"). In addition, it should be noted that the total strain energy also becomes insensitive to J_m as the magnification factor approaches to zero (see region "A" in Fig. 5). This will be discussed in the next section.

MULTIPLE JOINTS - Eq. (12) can be generalized to compute a derivative of the strain energy with respect to more than one joint stiffness. Given a group of joints which are of interest, the associated joint stiffness multiplier, α_p, is defined as:

$$(J_p, \ldots\ldots, J_{p+N}) = \alpha_p \, (\mathcal{J}_p, \ldots\ldots, \mathcal{J}_{p+N}) \tag{13}$$

The number of joints, N, in one group can be completely arbitrary. Then Eq. (10) can be modified as:

$$\frac{\partial U_s}{\partial \alpha_p} = \sum_{\ell=p}^{N} \left(1/2 \int_{V_\ell} \frac{\partial D_{jk}}{\partial \alpha_p} \, Q_j \, Q_k \, dV \right) \tag{14}$$

Again since $D_{jk} \propto 1/\alpha_p$, Eq. (14) becomes

$$\frac{\partial U_s}{\partial \alpha_p} = - \frac{1}{\alpha_p} \sum_{\ell=p}^{N} \left(1/2 \int_{V_\ell} D_{jk} \, Q_j \, Q_k \, dV \right) = - \frac{1}{\alpha_p} \sum_{\ell=p}^{N} U_\ell \tag{15}$$

Note that the individual strain energy has to be summed in this case. Therefore one can conclude that the following expression is also true:

$$\lim_{\alpha_p \to \infty} \frac{\partial U_s}{\partial \alpha_p} = 0 \tag{16}$$

Eq. (15) implies that the strain energy U_s is a hyperbolic function of the multiplication factor of the joint stiffnesses. Fig. 6 shows the total strain energy variation as functions of the multiplication factor, α_p. Again, the total strain energy becomes far less sensitive if α_p exceeds a certain value. This is the proof of the findings reported in Refs. [1] and [2].

DISCUSSION AND CONCLUSIONS

EFFECTS OF A SINGLE JOINT - When a single joint is varied, the overall vehicle stiffness becomes sensitive to the local joint stiffness only within a certain stiffness range (region "B", Fig. 5). In other words, the structure looses sensitivity not only when the magnification factor is small (region "A"), but also when the magnification factor is large (region "C"). The latter case has been proven in the previous section. For an explanation of the former case, one may consider the concept of a "failure mechanism" which has been used extensively in the literature on Limit Analysis [8]. Since the structure can sustain the given load with one or more "yield hinges", as long as the structure does not form a "mechanism", the structure can be said to have a finite stiffness, which is shown in the region "A" of Fig. 5. This means that, even if one removes the particular joint, the structure will still sustain a load within given limits.

EFFECTS OF MULTIPLE JOINTS - In the case of multiple joints, flexible joints have been introduced by adding 24 rotational spring elements at 12 structural joints in the model. The joints added in this fashion are shown in Fig. 4. A joint stiffness magnification factor (see α_p in Eq. (13)) was introduced and a parametric study of the joint behavior was performed. Fig. 6 shows a diagram of the total strain energy of the "stick" model versus the joint stiffness magnification factor for both bending and torsional loading cases. Published values for the joint stiffness obtained from three vehicle tests [9] (see Table 1) were used in the analyses. Table 2 as well as Fig. 6 compares the strain energy of the "stick" model (which has rigid joints) with strain energy computed using those three sets of joint stiffness. It is interesting to note that the strain energy values using the three sets of joint stiffness are all within a range of 3% and that those values, compared with the values of the "stick" model which has rigid joints, differ by a maximum of 11%. This means that the actual values of joint stiffness may be equal to or slightly smaller than the corresponding threshold values. Unlike in the case of a single joint, the total strain energy becomes infinitely large as the multiplication factor approaches to zero; this indicates that the joints shown in Fig. 4 may form a "failure mechanism".

"STICK" MODEL - These findings of the joints support the following hypothesis: A structure consisting of thin panels surrounded by frames, as is typical of automotive structures, may not be stiffened substantially by the panels under usual loading conditions, for the panels will buckle or deform like thin membranes, offering no support at the interior points. Even under these conditions, however, the part of the panel near the edge remains relatively undeformed, and acts as a gusset which stiffens the joint. This, then, implies the following modeling technique for the "stick" model of a vehicle structure: (i) The joints can be treated as rigid in the model, reflecting the fact that the panels act as gussets; this allows the joint stiffness to exceed the threshold value, and (ii) Since the panels contribute negligibly to the stiffness of the structure away from the joints, they do not have to be explicitly included in the model.

EFFECTS OF OTHER COMPONENTS - This idea, which has been applied to the joints, can be extended to other components. Similar phenomena can be seen by varying stiffness values of other components instead of varying those of just the joints. Figs. 7a and 7b show how the overall bending stiffness (solid lines) and torsional stiffness (dotted lines) change with the stiffness of the rocker panels or the tunnel. Figs. 7a and 7b were generated by varying the stiffness (abscissa) of the rocker panels and the tunnel, respectively. The ordinates represent the maximum deflections for bending and the twist angles for torsion, respectively. It is obvious from both Figs. 7a & 7b that the overall vehicle stiffness is much more sensitive to the rocker panel than to the tunnel under bending as well as torsional loadings. One can, however, see that the curves of both figures become flat as the stiffness of these two components increases. This phenomenon can also be shown using the equations derived in the previous section by replacing the variable b_m with the stiffness of either the rocker panels or the tunnel.

REFERENCES

1. Chang, D. C.: "Effects of Flexible Connections on Body Structural Response", SAE Transactions, Vol. 83, Paper No. 740071, pp 233-244, 1974.

2. Du, H. A. and Chon, C. T.: "Modeling of a Large-Scale Vehicle Structure", Proc. of the 8th Conf. on Electronic Computation, University of Houston, Houston, TX. ed. by J. K. Nelson Jr., ASCE, pp 326-335, 1983.

3. Chon, C. T.: "Design Sensitivity Analysis via Strain Energy Distribution", AIAA J. Vol. 22, No. 4, pp 559, 1984.

4. Chon, C. T. and Du, H. A.: "An Alternative Approach to Design Sensitivity Analysis for Large Scale Structures", Computers in Engineering, Vol. 3, ed. by D. E. Dietrich, pp 233, 1983.

5. DeVries, R. I. and Chon, C. T.: "Structural Design Sensitivity Analysis via Strain Energy Variations", 5th Int. Conf. on Vehicle Structural Mechanics, Detroit, MI. April 2-4, 1984, pp 135-141, 1984.

6. Malvern, L. E.: "Introduction to the Mechanics of a Continuous Medium", Prentice-Hall, Inc., Englewood Cliffs, N. J., 1969.

7. "MSC/NASTRAN - User's Manual", Version 62, ed. by C. W. McCormick, The MacNeal-Schwendler Corporation, April, 1982.

8. Hodge, P. G., Jr.: "Plastic Analysis of Structures", McGraw-Hill Book Co., N. Y., pp 20, 1959.

9. Crabb, H. C. et al,: "Structural Joint Performance", Advanced Structural & Safety Technology, Vehicle Development Technology, September 16, 1980.

TABLE 1.- MEASURED JOINT STIFFNESS VALUES.*

JOINTS	STIFFNESS ($x10^7$ N-mm/rad)		
	Vehicle A	Vehicle B	Vehicle C
1	2.12/1.61	3.96/3.48	5.12/3.38
2	3.55/2.46	2.45/3.69	3.48/2.84
3	14.4/3.92	28.7/15.6	18.0/5.14
4	20.1/3.26	39.3/4.51	27.4/4.12
5	2.35/0.18	2.75/0.12	7.41/0.20
6	10.1/0.54	22.6/1.25	16.9/1.29

(Fore-Aft/In-Outboard)

*(See Fig. 4 for corresponding joint numbers.)

TABLE 2.- COMPARISON OF STRAIN ENERGIES OF "STICK" MODEL AND STRAIN ENERGY COMPUTED USING JOINT STIFFNESS LISTED IN TABLE 1.

STRAIN ENERGY	BENDING	TORSION
U ("STICK" MODEL)	$7.04x10^3$ (1.00)	$2.88x10^4$ (1.00)
U (Vehicle A)	$7.79x10^3$ (1.11)	$3.17x10^4$ (1.10)
U (Vehicle B)	$7.69x10^3$ (1.09)	$3.07x10^4$ (1.07)
U (Vehicle C)	$7.57x10^3$ (1.08)	$3.11x10^4$ (1.08)

N-mm

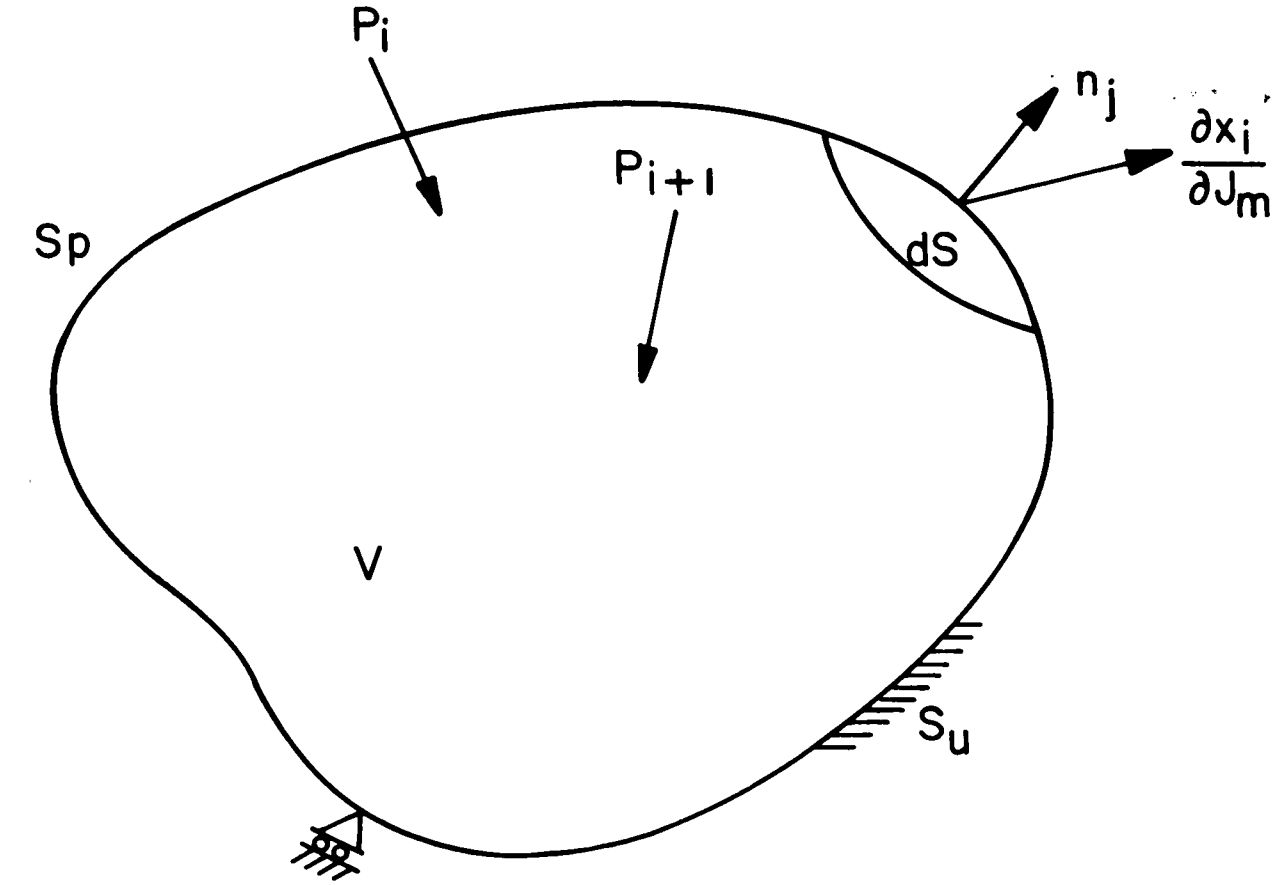

Figure 1 - A general body surface S consists of two parts, S_p and S_u. Over S_p, forces are prescribed and over S_u, displacements are prescribed. The term n is the unit vector normal to the surface.

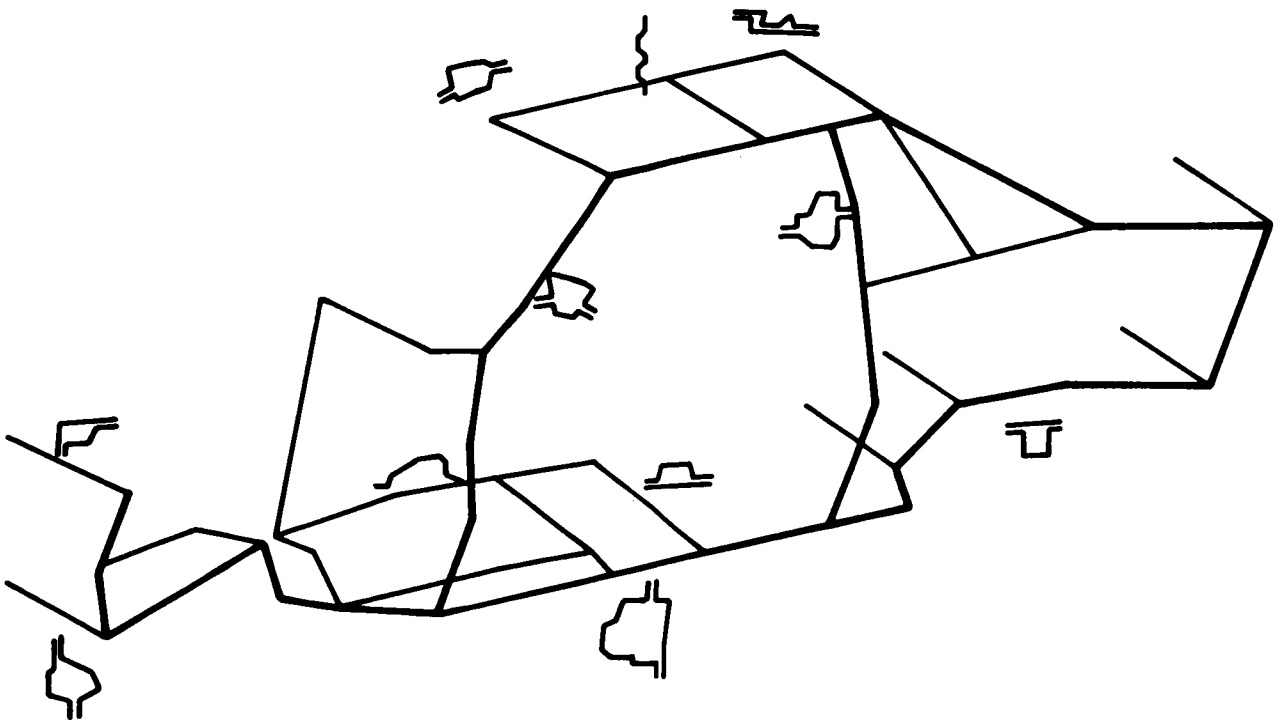

Figure 2 - A typical "STICK" model with cross-sectional shapes of beam elements.

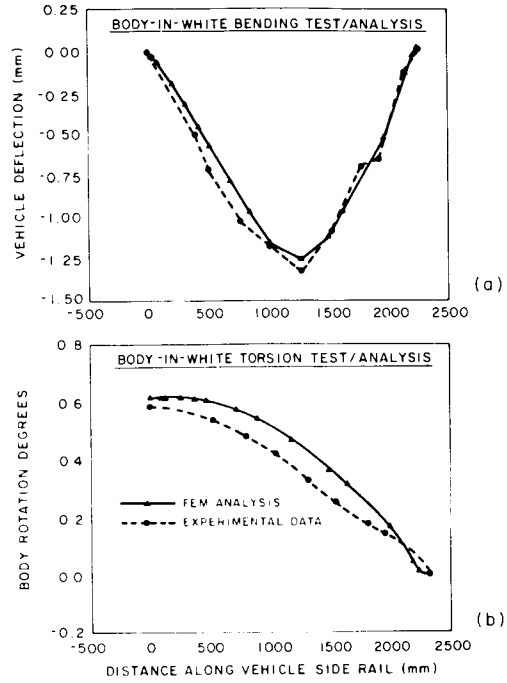

Figure 3 - Deflection versus wheel base length a "STICK" model for bending and torsion. Solid and dotted lines represent analytical results and test data, respectively.

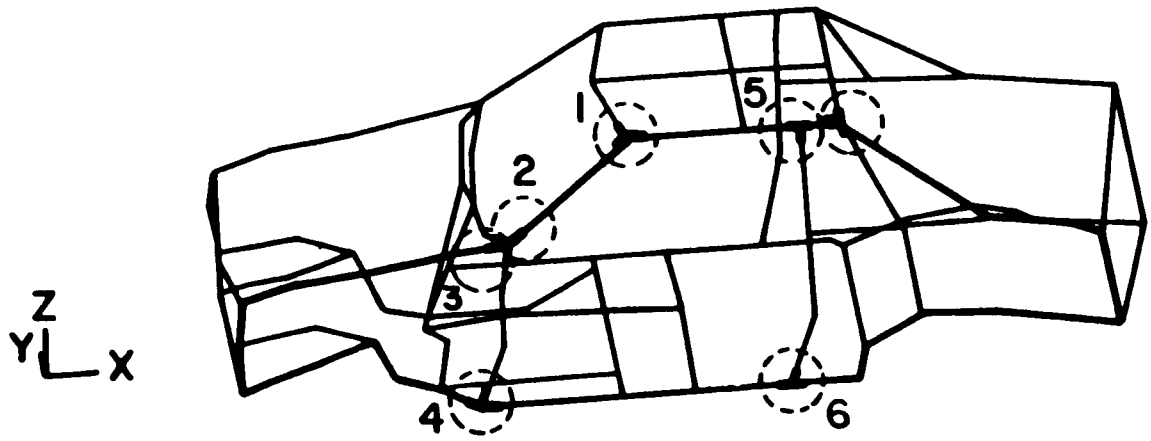

1) A-PILLAR TO ROOF RAIL
2) A-PILLAR TO FRT HINGE PILLAR
3) SHOTGUN TO FRT HINGE PILLAR
4) FRT HINGE PILLAR TO ROCKER
5) B-PILLAR TO ROOF RAIL
6) B-PILLAR TO ROCKER

Figure 4 - Joint locations.

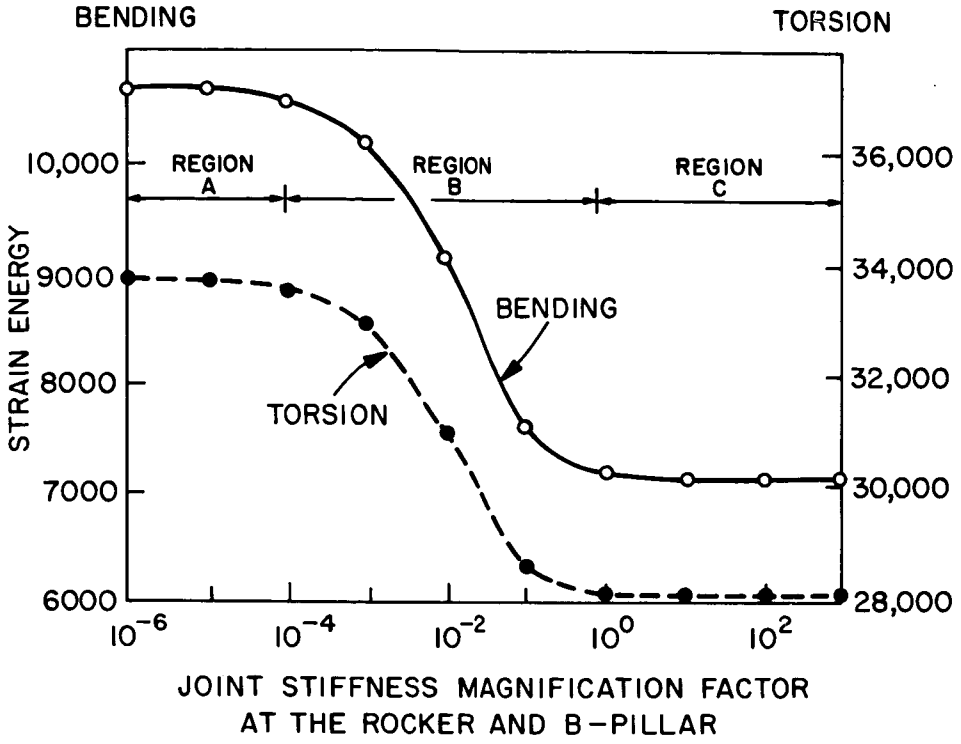

Figure 5 - Strain energy versus stiffness of the joint between the rocker panels and the B-pillar.

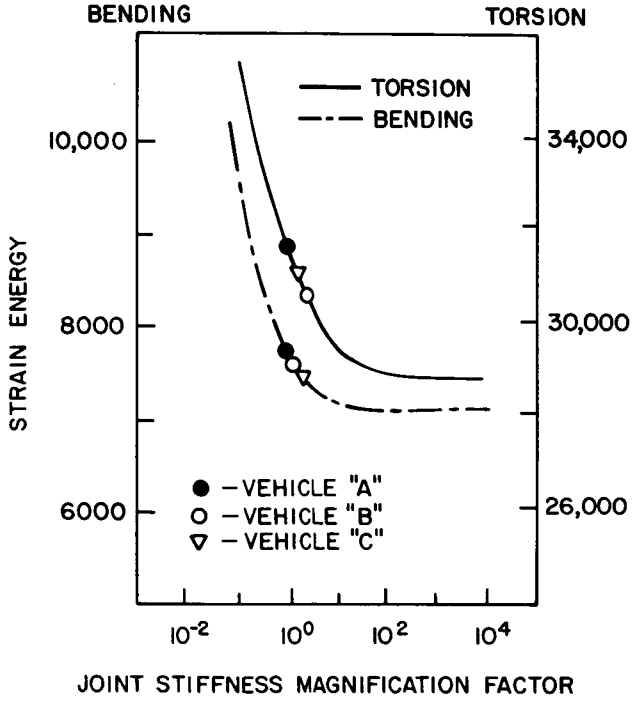

Figure 6 - Strain energy versus joint stiffness magnification factor. Strain energy obtained using measured joint stiffnesses from three vehicle structures is also shown.

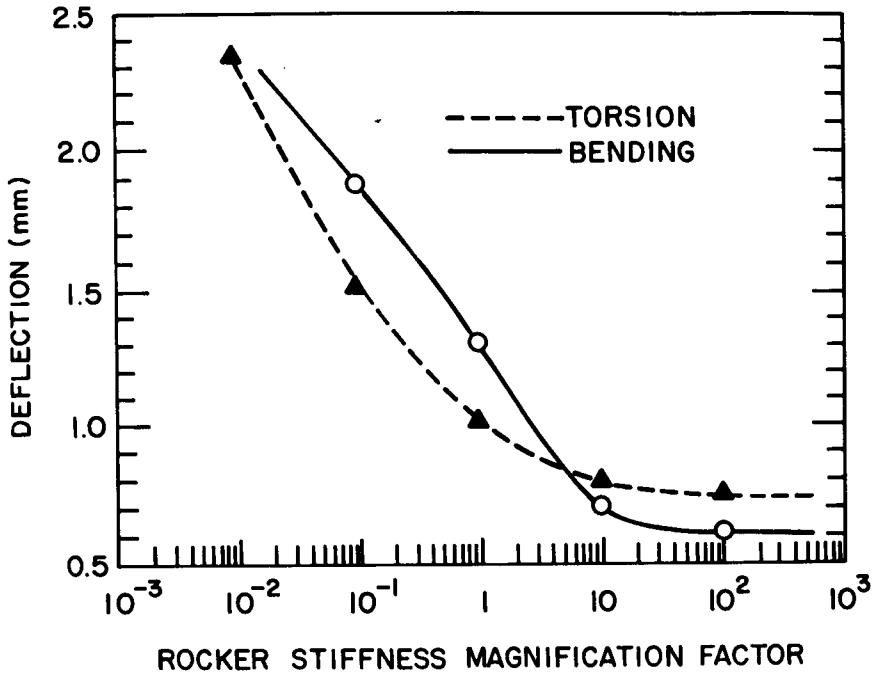

a - Maximum deflection versus rocker stiffness magnification factor.

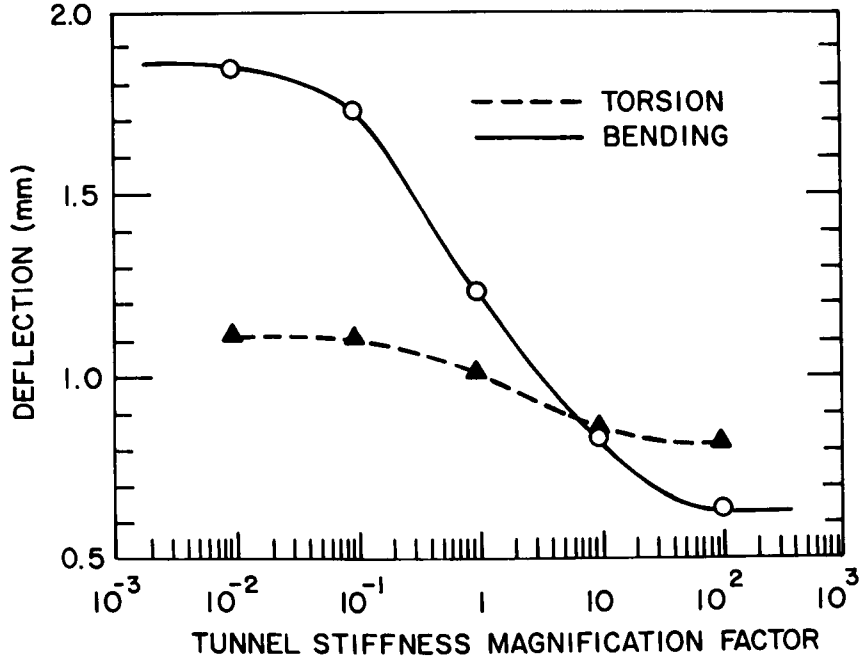

b - Maximum deflection versus tunnel stiffness magnification factor.

Figure 7 - Maximum deflections versus rocker stiffness and tunnel stiffness magnification factor.